Journal of Applied Polymer Science

Synthesis and Characterization of a Chitosan Ligand for the Removal of Copper from Aqueous Media

Desireddy Harikishore Kumar Reddy, Seung-Mok Lee
Department of Environmental Engineering, Kwandong University, 522 Naegok-Dong, Gangneung-Si, Gangwon-Do 210-701, Republic of Korea
Correspondence to: S.-M. Lee (E-mail: leesm@kwandong.ac.kr)

ABSTRACT: A novel chitosan derivative, 8-hydroxyquinioline-2-carboxaldehydechitosan (CSHQ) Schiff base, was synthesized by a simple condensation process. The structure of the resulting product was confirmed by Fourier transform infrared spectroscopy, solid-state ^{13}C-NMR, differential scanning calorimetry, scanning electron microscopy, and energy-dispersive X-ray spectroscopy. Further, the synthesized CSHQ Schiff base was used as an adsorbent for the removal of Cu(II) from aqueous solution. The adsorption of Cu(II) onto CSHQ was strongly dependent on the pH value, and the optimum pH value obtained was pH 5. Among the pseudo-first-order (PFO), pseudo-second-order (PSO), and intraparticle diffusion model simulation, the experimental data followed PSO kinetics well. The Cu(II) adsorption process onto CSHQ obeyed the Langmuir isotherm model well rather than the Freundlich and Sips isotherm models; this suggested that a monolayer adsorption occurred on the surface of CSHQ. From the overall results, we found that Cu(II) was adsorbed onto CSHQ through oxygne, nitrogen and pyridine nitrogen donor atoms and that CSHQ could be a promising adsorbent for water treatment. © 2013 Wiley Periodicals, Inc. J. Appl. Polym. Sci. 000: 000–000, 2013

KEYWORDS: adsorption; copolymers; crosslinking; kinetics; separation techniques

Received 26 December 2012; accepted 16 May 2013; Published online
DOI: 10.1002/app.39578

INTRODUCTION

Copper is an essential micronutrient and is vital for all living organisms; however, several health issues arise when it is deficient or in excess.[1,2] An excessive intake of copper results in many side effects and health risks, including stomach and intestine problems, mucosal irritation, kidney failure, neurotoxicity, and Wilson disease.[3–6] Copper is among the most common heavy metals that are often present in industrial effluents, such as metal cleaning and plating baths; the electroplating industry; brass manufacturing; pulp, paper and paperboard mills; wood pulp production; and copper-based agrichemicals.[7] Hence, the removal of copper from water and wastewater is deemed to be of paramount importance in the protection of the aquatic environment. Many technologies have been developed to remove copper from contaminated waters. However, because of its efficiency and economic feasibility, adsorption has become an alternative method for the removal of various toxic pollutants, including copper from the aqueous effluent. A number of low-cost adsorbents produced from many raw materials, such as agricultural and industrial waste, have been of great interest for this purpose. A few interesting low-cost adsorbents have been reported in the literature; these include apple waste,[8] sawdust,[9] sewage sludge,[10] and honeycomb,[11] which have been employed for treating copper-contaminated aqueous systems.

In recent years, biopolymers derived from renewable resources, mainly polysaccharides, have initiated extensive interest in the field of water treatment because of their low-cost, availability, and the advantageous presence of various chelating functional groups.[12] Among them, chitosan (CS) is economically attractive and is the second most abundant polysaccharide existing in nature; it plays a prominent role in the detoxification of wastewater because of the presence of high contents of amino and hydroxyl functional groups.[12–15] CS and its derivatives/composites have been reported to be suitable materials for removing a number of chemical species: metal ions,[16–18] dyes,[19,20] ammonia,[21] humic acid,[22] protein,[23] fluoride,[24] phenols,[15] and several other pollutants. However, pure CS is very sensitive to the pH of ionic solutions; it can be dissolved under acidic conditions because of the intermolecular and intramolecular hydrogen bonding. Along with this, CS has a few other disadvantages,

Additional Supporting Information may be found in the online version of this article.

including poor chemical resistance, low mechanical strength, and severe shrinkage and deformation after drying.[25–27] Although CS by itself is a good adsorbent, these drawbacks have hindered the application of pure CS in chemically and physically harsh environments.

To resolve such problems, various efforts have been focused in recent years on the development of chemically and mechanically stable CS derivatives. From this perspective, several researchers have used crosslinking agents, such as glyoxal, formaldehyde, glutaraldehyde, epichlorohydrin, ethylene glycol diglycidyl ether, and isocyanates, to stabilize and enhance the mechanical properties of CS.[19,28,29] Although this crosslinking technique may enhance the resistance of CS against acids, the process may minimize its adsorption capacity when used to treat wastewater. This is because of the fact that the amino groups of CS, which play a great part in the adsorption process, are involved in crosslinking. On the basis of the aforementioned reasons and because of its polyfunctionality,[30] CS has been modified by various chelating functional groups to facilitate the introduction of additional donor atoms, to enhance its adsorption performance, and to overcome the various disadvantages of pure CS.[31] In this sense, the preparation of functionalized CS derivatives (which can offer more functional groups and chemical stability) has become a key research area for the development of novel chelating ligands and has stimulated intense research on highly efficient CS ligands. In this sense, the modification of primary amines in the polymeric chain of CS with aldehydes or ketones to synthesize Schiff bases (—RC═N—) has gained much attention.[32–34] In addition, as-prepared CS Schiff bases are able to form stable complexes with metal ions and are useful for several analytical and environmental applications.[35,36] Numerous studies on CS Schiff bases and their use for the removal of various metal ions, including lanthanides, actinides, noble metals, and transition-metal ions, are available in the literature.[37–39] On the basis of the previous considerations, in this study, we used a new chelating agent, 8-hydroxyquinoline-2-carboxaldehyde (HQC), to synthesize a CS Schiff-base compound. It is well-known from the literature that Schiff-base ligands synthesized from HQC have a strong ability to form metal complexes with Cu(II) and other metal ions.[40–43] To our knowledge, this is the first report on the preparation of a CS Schiff base with HQC and its application for removing Cu(II) from aqueous solutions.

In this article, we describe the synthesis of a novel CS Schiff base with HQC and CS in a simple condensation process. Further, we discuss the complete characterization of the ligand, together with Cu(II) removal from aqueous solution. Batch adsorption studies were carried out to investigate various parameters, including the effects of pH, contact time, and initial concentration, on copper removal. We found that a pseudo-second-order (PSO) equation was best fitted to the kinetic data, and the adsorption equilibrium data was well fitted to the Langmuir isotherm.

EXPERIMENTAL

Materials

HQC (catalog number 55083) and CS (catalog number 44,8869, low molecular weight with deacetylation percentage in the range of 75–85%) were purchased from Sigma-Aldrich and used without further purification. All solvents and other reagents used in this experiment were of analytical reagent grade.

Synthesis of 8-Hydroxyquinioline-2-Carboxaldehydechitosan (CSHQ)

The new CS Schiff-base ligand was derived by simple condensation of CS with HQC. In a typical synthesis, CS powder (1.0 g) was first dissolved in 25 mL of 1 wt % acetic acid, and then it was diluted with methanol (100 mL). Then 1 g of 8-hydroxyquinoline carboxaldehyde dissolved in methanol (20 mL) was added slowly. The mixture was stirred at room temperature for 16 h; this was followed by refluxing for 18 h, which resulted in a yellow solid. The solid was then decanted, thoroughly washed with methanol to remove any unreacted ligand, and then dried *in vacuo* at 60°C. This modified CS derivative was named CSHQ and was used for further studies.

Analytical Methods

Fourier transform infrared (FTIR) spectra of the derivative were measured in the 4000–400-cm^{-1} region with a Bruker Tensor 27 instrument by the KBr disk method. Solid-state ^{13}C-NMR spectra were obtained from a Bruker DSX 300 spectrometer. The thermal behavior of CS and its derivative were studied with a Mettler-Toledo differential scanning calorimeter. The samples were accurately weighed, put into aluminum pans, and then sealed with aluminum lids. An empty pan was used as the reference in this test. The thermograms of the samples were obtained at a scanning rate of 20°C/min over a temperature range of 10–500°C. The morphologies and elemental compositions were obtained with a scanning electron microscopy (SEM) machine (field emission SEM instrument, model SU-70, Hitachi, Tokyo, Japan) equipped with an energy-dispersive X-ray spectroscopy (EDX) system.

Batch Adsorption Experiments

Batch experiments were carried out to determine the effect of different operational variables, namely, the pH, equilibrium time, and initial concentration. All of the batch experiments were performed with a solution of Cu(II) (50 mL, 50 mg/L initial concentration) at 303 K, unless otherwise noted, with 50 mg of the sorbent CSHQ. To investigate the effect of the contact time, the initial pH of the testing solutions was chosen from the optimal pH value, which resulted in a high adsorption of the metal ions. The solutions were held in an airtight stoppered conical flask (100 mL) in a thermostatic shaker bath, operating at 303 K. The initial pH of the testing solution was adjusted with either a 0.1*M* HCl or 0.1*M* NaOH aqueous solution. The equilibrium sorption capacity (q_e) was calculated as follows:

$$q_e = \frac{V(C_0 - C_e)}{m}$$

where q_e is the metal-ion uptake capacity of the adsorbent at equilibrium; V is the sample volume (mL); C_0 and C_e represent the concentration of Cu(II) before and after the removal process, respectively; and m is the weight of the adsorbent.

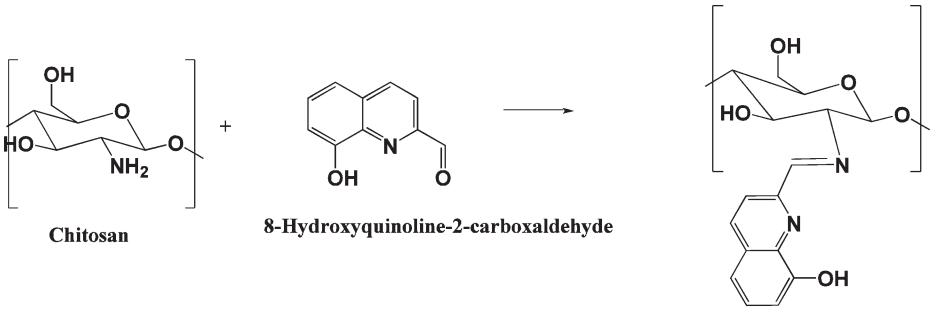

Scheme 1. Synthesis of the novel CS derivative CSHQ.

RESULTS AND DISCUSSION

The new CS derivative CSHQ was synthesized by the simple condensation of CS with equivalent amounts of HQC. In the preparation of CSHQ, CS acted as a primary amine and reacted with the aldehyde group of HQC and provided Schiff-base formation in the polymeric structure, as shown in Scheme 1. The ligand HQC introduced new coordination groups into CS, such as hydroxyl (OH), imine (═N), pyridine nitrogen (—N) groups. In this new ONN (oxygen, nitrogen and nitrogen) tridentate system, an O atom, N atom are from HQC and an azomethine N atom from chitosan. These atoms were able to form stable complexes with a wide variety of metal ions.

Characterization of CSHQ

FTIR Spectral Analysis. The FTIR spectra of CS and its new derivative are shown in Figure 1. The FTIR spectrum of CS exhibited a broad peak around 3469 cm^{-1} corresponding to γ(OH) stretching; this was superimposed with the N—H stretching band. The weak band at 2900 cm^{-1} was the characteristic axial stretching of the C—H group; in addition, a peak around 1420 cm^{-1} due to CH_2 scissoring was also identified.[44] Further, absorption peaks observed at 1590 and 1654 cm^{-1} were assigned to N—H bending vibrations of the secondary amide. The absorption band at a wave number of 1379 cm^{-1} corresponded to the C—O stretching of the amide group. Additionally, the absorption peaks of the symmetric stretching of C—O—C appeared at 1152 and 1070 cm^{-1}. When the FTIR spectra of CS and CSHQ were first compared, we observed an obvious change between 3500 and 3200 cm^{-1} due to the O—H and N—H group stretching vibrations. In addition, the peak at 1590 cm^{-1} of the amino groups of CS disappeared; this meant that the amino group was substituted. A comparison of CS with CSHQ showed a significant peak at 1647 cm^{-1}, which was attributed to the C═N formed by the reaction between the amino group and the aldehyde group. In addition to this, a characteristic absorption peak at 1590 cm^{-1} almost disappeared; this indicated the formation of the Schiff base. The band around 1570 cm^{-1} in the spectra of CSHQ was assigned to γ(C═N) of pyridine.[41]

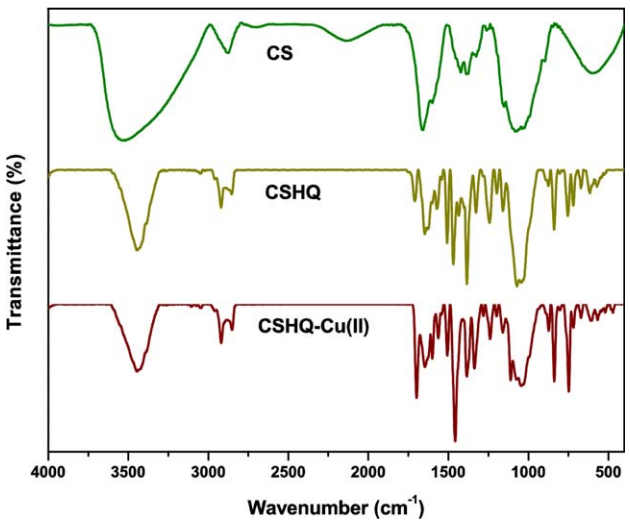

Figure 1. FTIR spectra of CS, CSHQ, and Cu(II)-loaded CSHQ. [Color figure can be viewed in the online issue, which is available at wileyonlinelibrary.com.]

Solid-State ^{13}C-NMR Spectra. To further verify the findings from the FTIR spectra, solid-state ^{13}C-NMR analysis was carried to confirm the structure of CS and its derivative. The spectra of CS and CSHQ are shown in Figure 1 in the Supporting Information. CS had the expected signals, as numbered in the structural representations on the left-hand side in the figure, and coincided with a ^{13}C-NMR spectra reported previously.[45] In the case of CSHQ, we observed that a new signal for substituted C2 appeared at 61 ppm. This confirmed that some of the aminos at C2 were substituted further; a signal appeared at 166.09 ppm, which indicated the formation of the Schiff base. Further, a few additional peaks were observed in the region 112–175 ppm; these were due to the presence of aromatic carbon atoms in the CS derivative.[46] The ^{13}C-NMR spectrum further confirmed that the new CS derivative (CSHQ) was successfully synthetized.

Differential Scanning Calorimetry (DSC). The thermal characterization of CS and its new derivative was performed with the DSC technique, and Figure 2 presents the corresponding thermograms. As shown in the figure, both CS and CSHQ had a two-stage degradation pattern in the DSC thermograms. CS showed an endothermic peak at 73.84°C and a sharp exothermic peak at 304.22°C. The former endothermic peak may have been due to the thermal evaporation of bound water that could not be removed completely upon drying, whereas the latter exothermic peak could be attributed to the thermal decomposition of the CS biopolymer. The thermogram of CSHQ showed an endothermic peak at 77.58°C, which was associated with the loss of water from the CSHQ. The

Applied Polymer SCIENCE

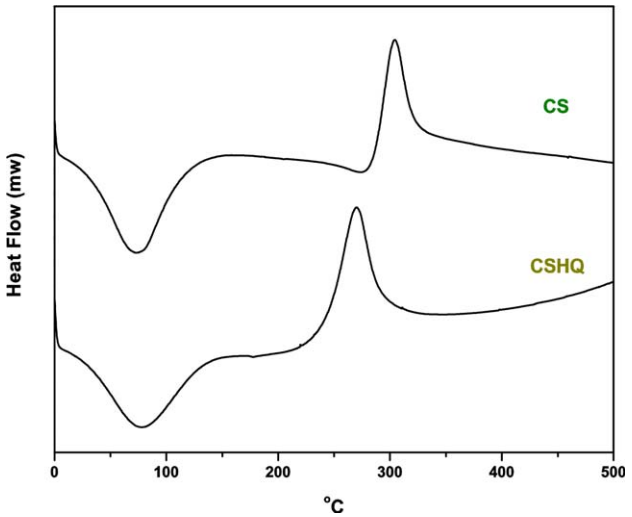

Figure 2. DSC curves of CS and CSHQ. [Color figure can be viewed in the online issue, which is available at wileyonlinelibrary.com.]

decomposition peak (exothermic peak) at 270.13°C corresponded to the thermal degradation of CSHQ and was slightly lower than that of CS (304.22°C) with little dependence on the type of substituents on the aromatic ring, and the intensity of these peak decreased. The results indicate that a significant difference in the position of the exothermic peaks of CS and CSHQ was observed; this confirmed the formation the new CS derivative (CSHQ).

Microscopic Analysis. The morphology of CS and its derivative CSHQ were analyzed with SEM, as shown in Figure 2 in the Supporting Information. The native CS exhibited an irregular flake surface and a flat morphology with no pores;[47] this may have been due to high density of intermolecular hydrogen bonds of CS.[48] The nonuniform particles were due to the uneven size of the CS flakes. However, the morphology of CS was affected. After modification with HQC, conspicuous morphological changes were observed, and CSHQ exhibited a more compact and rigid structure. CS had a smooth surface, whereas CSHQ showed a rougher surface; this may have been due to the reaction of the ligand HQC with CS. This difference shows that CS was successfully modified by HQC.

Effect of the Solution pH on Adsorption

The solution pH was a vital parameter and significantly influenced the degree of ionization and speciation of metal ions in aqueous solution. To describe the binding of Cu(II) onto CSHQ, first the speciation and solubility of Cu(II) was studied. The visual MEDUSA speciation program was used to calculate the molar fractions of copper ions. The copper speciation diagram demonstrated the concentration of dissolved species and the pH at which hydrolysis occurred (Figure 3, Supporting Information). It was observed that copper predominantly existed as Cu^{2+} and $CuOH^{+}$ cations within the pH range 2.0–5.8. A number of other ionic forms, such as $Cu_2OH_3^{+}$, $Cu(OH)_2$, $Cu_2(OH)_2^{2+}$, and CuO, were present in solution between pH 5.0 and pH 8.0. The concentration of Cu(II) started to decrease at $pH > 6.0$ due to precipitation.

To evaluate the effect of pH on the adsorption of Cu(II) ions, experiments were carried out with different initial pHs ranging from 2.0 to 8.0. The effect of the initial solution pH on Cu(II) removal is presented in Figure 3, and we observed that the removal of Cu(II) ions was clearly pH-dependent. In general, the hydrogen ion concentration played a significant role on the adsorption of metal ions from aqueous solution when CS and its derivative was used for this purpose. Under acidic conditions (pH 2–3), most of the active sites present in CSHQ were ionized and present in the protonated form; thus, metal-ion removal was low at these pHs. In addition, the competitive adsorption between the prevalently available H^{+} and the metal ions resulted in a lower adsorption. The removal was increased with increasing pH value from 3 to 5 and reached a plateau at pH 5.0 and 6.0. Further, there was no significant increase in the removal up to pH 8.0. The increase in the percentage removal with increasing pH may have been due to the presence of a free lone pair of electrons on nitrogen atoms suitable for coordination with the metal ion. In addition to the elevation of the solution pH, deprotonation took place at the hydroxyl groups present in CSHQ. Consequently, an amount of coordination between the hydroxyl groups with copper ions was possible, and this resulted in a high removal percentage. Also, the final pH values after adsorption were determined and are presented in Figure 3. The final pH values increased slightly with initial pH values up to pH 3 and decreased above this pH value. A possible reason for the decrease in the pH value after adsorption have been the deprotonation of the adsorbent surface. From these results, we concluded that CSHQ had a wider suitable pH range (from pH 4.0 to pH 7.0), and this could broaden its application areas. To preserve the metal in solution, an initial pH of 5 was chosen as the optimum value in further equilibrium and kinetic experiments.

Adsorption Kinetics of Cu(II) on CSHQ

Adsorption is a time-dependent process, and predicting the rate at which adsorption takes place for a given system is one of the most important characteristics for the design and evaluation of an adsorbent.[49] To establish the rate law of adsorbate–adsorbent

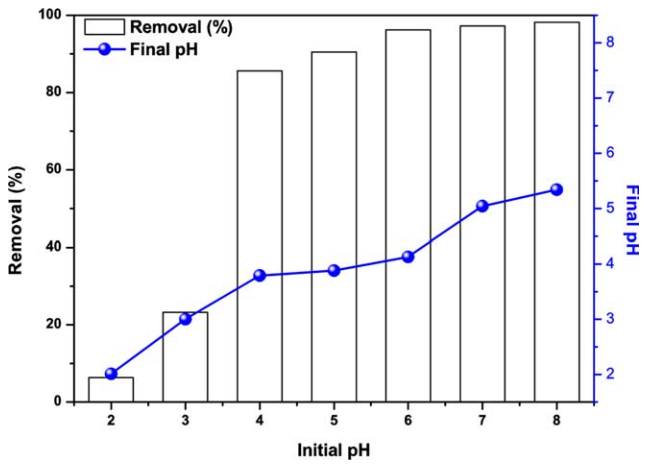

Figure 3. Removal percentage of Cu(II) onto CSHQ as a function of the pH. [Color figure can be viewed in the online issue, which is available at wileyonlinelibrary.com.]

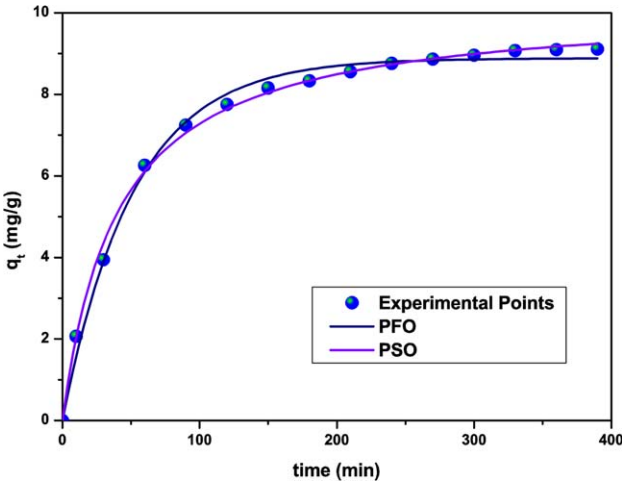

Figure 4. PFO and PSO nonlinear kinetic models for Cu(II) removal onto CSHQ. [Color figure can be viewed in the online issue, which is available at wileyonlinelibrary.com.]

interactions, the application of adsorption kinetic modeling is essential. The adsorption kinetics can be analyzed with several models; however, the pseudo-first-order (PFO),[50] pseudo-second-order (PSO),[51,52] and Weber–Morris[53] models have been widely used to investigate the adsorption of metal ions onto CS and its derivatives. As shown in Figure 4, the adsorption amount increased with increasing contact time and reached equilibria within 6 h.

The PFO, PSO, and Weber–Morris models were used to simulate the adsorption kinetics of Cu(II) onto CSHQ. The kinetic parameters, along with the correlation coefficients (R^2s), from the nonlinear fitting of the data for the PFO and PSO kinetic models are listed in Table I. By contrast, the PSO model described the experimental data pretty well (Figure 4). Also, the high R^2 and low χ^2 values for the PSO kinetic model compared to the PFO kinetic model reinforced the applicability of the PSO model. We made a comparison by plotting the graph

Table I. Kinetic Parameters of the PFO and PSO Models for the Removal of Copper by CSHQ

Model	Parameters and goodness of fit	Parameter values
Pseudo-first-order $q_t = q_e(1-e^{-k_1 t})$	$q_{e,Calcd}$ (mg/g^{-1})	8.885
	k_1 (min^{-1})	0.019
	χ^2	0.052
	R^2	0.9935
Pseudo-second-order $q_t = q_e \frac{q_e k_2 t}{1+q_e k_2 t}$	$q_{e,Cal}$ (mg/g^{-1})	10.195
	k_2 (g mg^{-1} min^{-1})	0.002
	h (mg g^{-1} min^{-1})	0.207
	χ^2	0.022
	R^2	0.9947

k_1, rate constant of the first-order kinetic model; k_2, rate constant of the second-order kinetic model; t, time (min), h, initial sorption rate.

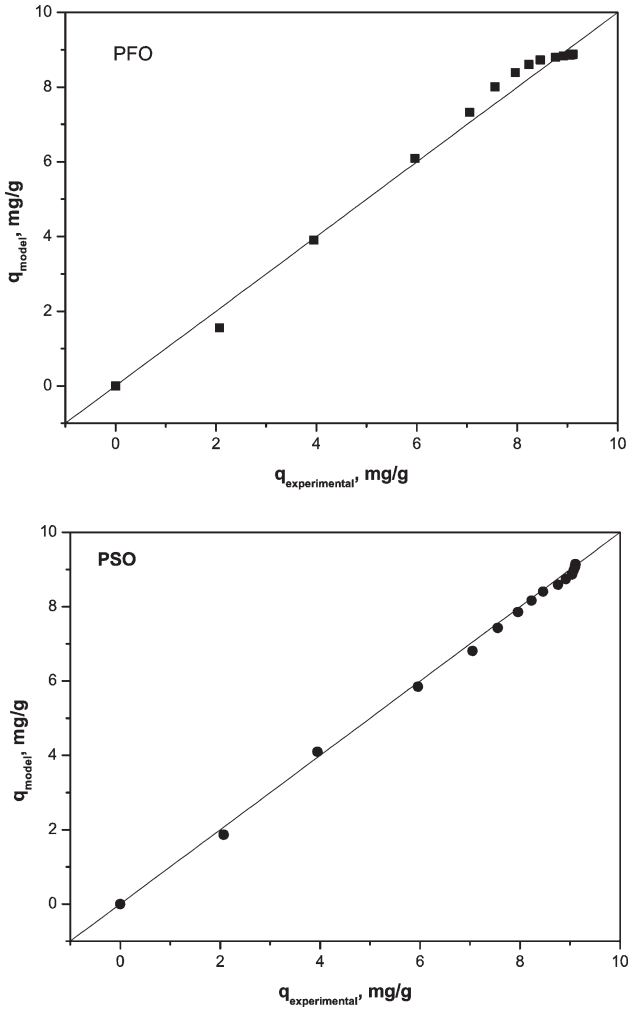

Figure 5. Comparison of the $q_{experimental}$ and q_{model} values of Cu(II) removal onto CSHQ for the PFO and PSO kinetic models.

between the experimental and calculated q_e values of Cu(II) adsorption onto CSHQ to identify the choice of the PFO and PSO models (Figure 5). We observed that for the PSO model, most of the data were distributed around the 45° line compared with the PFO model; this indicated that the PSO model satisfactorily described the experimental data with the obtained model values. Therefore, the sorption reaction could be approximated more favorably by the PSO kinetic model, and the superior conformity of the PSO model indicated the chemical nature of the interactions between the Cu(II) ions and CSHQ.

To investigate the contribution of the surface and intraparticle diffusion on the overall adsorption process, the sorption kinetic data was processed with the empirical relationship based on the Weber–Morris model (Table II). If intraparticle diffusion is assumed to be the sole rate-controlling step, a plot of q_e versus $t^{1/2}$ should yield a straight line passing through the origin.[54] As shown in Figure 6, the intraparticle diffusion plot did not pass through the origin and exhibited trilinearity in the adsorption process; this indicated that the three steps taking place were operational. The first linear portion included the sorption period of 0–150 min, attributed to the external mass transfer

Table II. Parameters of the Weber–Morris Model for the Removal of Copper by CSHQ

Weber–Morris model	Parameters and goodness of fit	Parameter values for the three stages		
		I	II	III
$q=K_i t^{1/2}+C$	K_{id} (mg g^{-1} min$^{0.5}$)	0.664	0.233	0.055
	C (mg/g)	0.323	5.092	8.048
	R^2	0.9624	0.9937	0.7829

K_{id}, Weber–Morris kinetic constant; q, amount of adsorbate adsorbed (mg/g); C, intercept from the Weber–Morris equation.

(external diffusion); the second linear portion between 150 and 270 min described the intraparticle diffusion, and the third linear portion included the time period 270–390 min, a plateau to equilibrium. The intraparticle diffusion coefficient for the sorption of Cu(II) was calculated from the slope of the plot between the amount of Cu(II) sorbed (q_t; mg/g) versus $t^{1/2}$, as presented in Table II. The values of R^2 for the intraparticle diffusion model were lower than that for the PSO model.

Adsorption Isotherms

The equilibrium adsorption isotherms are important data for understanding the adsorption mechanism and are important in the design of an adsorption system. In this investigation, the experimental equilibrium data for the adsorption of Cu(II) on CSHQ with various initial concentrations was fitted with three well-known Langmuir and Freundlich two-parameter models and the three-parameter Sips model to evaluate the adsorption phenomenon. A relatively high R^2 and low χ^2 values were used to identify the suitable isotherm for adsorption of Cu(II) onto CSHQ. The parameter isotherm models and R^2s were calculated with Origin 8.0 software by plotting the values of C_e versus q_e, and the results are presented in Table III.

This table shows that the Langmuir isotherm model[55] fit the equilibrium data very well with a high R^2 (0.999) and low χ^2 values (0.184). This meant that even when different active sites were available on CSHQ, they were distributed homogeneously on the surface of CSHQ because the Langmuir equation assumes that the surface is homogeneous.[55] The maximum adsorption capacity obtained from the Langmuir isotherm model was 88.07 mg/g. The essential features of a Langmuir isotherm can be expressed in terms of a dimensionless constant separation factor (R_L), which is defined as $R_L = 1/1 + K_L C_0$.[56] The calculated R_L values were greater than zero and less than unity (0.20–0.60), which confirmed a favorable adsorption process for Cu(II) removal with CSHQ. This means that the equilibrium isotherms could be well described by the Langmuir model. The Freundlich isotherm model[57] is used for affinities over the heterogeneous surface energy systems and for describing a multilayer adsorption system with interactions between adsorbed molecules.[58] The lower R^2 and high χ^2 values obtained in the case of the Freundlich isotherm model indicated that the Freundlich isotherm model was not adequate to describe the adsorption process of Cu(II) onto CSHQ. To describe a more complex adsorption behavior, both the Langmuir and Freundlich isotherms were combined in the Langmuir–Freundlich

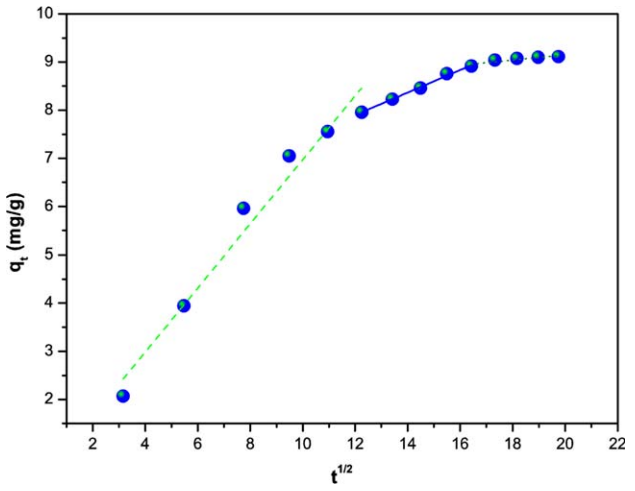

Figure 6. Weber–Morris model (stages of intraparticle diffusion) for Cu(II) adsorption onto CSHQ. [Color figure can be viewed in the online issue, which is available at wileyonlinelibrary.com.]

Table III. Isotherm Parameter Constants for Cu(II) Adsorption onto CSHQ

Model	Parameters and goodness of fit	Parameter value
Langmuir $q_e=\frac{q_{max}K_L c_e}{1+K_L c_e}$	q_{max}	88.070
	K_L	0.026
	χ^2	0.184
	R^2	0.9993
Freundlich $q_e=K_F C_e^{1/n}$	K_F	6.790
	$1/n_F$	0.501
	χ^2	7.486
	R^2	0.9745
Langmuir–Freundlich (Sips) $q=q_{max}\frac{b_{LF}.C_e^{nLF}}{1+b_{LF}.C_e^{nLF}}$	q_{max}	87.226
	n_{LF}	1.010
	χ^2	0.241
	R^2	0.9991

K_L, Langmuir isotherm constant (dm^3/mg); K_F, Freundlich isotherm constant [(mg g^{-1})(L mg^{-1})$^{1/n_F}$]; q, amount of adsorbate adsorbed (mg/g); q_{max}, maximum biosorption capacity (mg/g); b_{LF}, Langmuir–Freundlich isotherm constant (dm^3/mg); nF, exponent in Freundlich isotherm; nLF, exponent in Langmuir-Freundlich isotherm.

Table IV. Comparison of the Adsorption Capacities of Various CS-Based Adsorbents

Adsorbent	q_{max} (mg/g)	pH	Reference
N-(4-Pyridylmethyl) chitosan	45.1	7.6	35
CCTSL	82.64	8.5	37
CTSL	56.8	8.5	38
Carboxylated CS beads	86.0	6.0	60
Epichlorohydrine chitosan	62.47	6.0	61
CS modified with Reactive Orange 16 dye	107.3	5.5	62
CHS-BPMAMF	109	5.5	63
CTS-ECH-TPP	130.72	6.0	64
ECXCs	43.47	5.0	65
CSHQ	88.07	5.0	This study

CHS-BPMAMF, chitosan biopolymer chemically modified with the complexation agent 2[bis(pyridylmethyl)aminomethyl]-4-methyl-6-formylphenol; CTS-ECH-TPP, chitosan crosslinked with epichlorohydrin and triphosphate; ECXCs, epichlorohydrin crosslinked xanthate chitosan; CCTSL, crosslinked chitosan derivative; CTSL, chitosan biopolymer derivative.

(Sips)[59] model after the Langmuir model at high concentrations and the Freundlich model at low concentrations of adsorbate. Further, the n_{LF} (exponent in LangmuirFreundlich isotherm) value of the Sips isotherm model was close to unity, and this indicated that the adsorbent had homogeneous binding sites. n_{LF} for the adsorption of Cu(II) was 1.010, as confirmed by the Langmuir isotherm, which assumes homogeneous adsorption.

The values of R^2 and χ^2 showed that the three isotherm models descended in the order Langmuir > Sips > Freundlich. It is noteworthy that the Langmuir model was found to describe adsorption, and this suggested that adsorption took place on a homogeneous surface by monolayer sorption.

Comparison of the Maximum Adsorption Capacities of CSHQ and Other Adsorbents

A comparison of the maximum adsorption capacities of CSHQ for the removal of Cu(II) was done with those of other chemically modified CS derivatives reported in the literature, and this comparison is illustrated in Table IV. The reported maximum adsorption capacities were based on the Langmuir isotherm model. The maximum Cu(II) adsorption capacity (88.07 mg/g) by CSHQ at the optimum pH 5.0 was comparable with those of previously reported CS derivatives. The comparison of the maximum adsorption capacities of various CS adsorbents with CSHQ revealed that CSHQ exhibited a higher adsorption capacity than other reported CS derivatives, and it showed a lower adsorption capacity than few CS adsorbents. The reason for difference in the adsorption capacities may have been the different experimental conditions and the available functional groups on the adsorbents. However, more important was that CSHQ was prepared in the absence of crosslinking agents, which were used in the case of a few CS derivatives that exhibited higher adsorption capacities. Further, CSHQ was obtained in a simple condensation process. This gave advantages in terms of the chemical and process costs; thus, CSHQ could be effectively used as an adsorbent for the removal of copper ions from aqueous solutions.

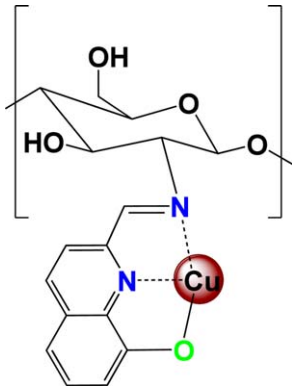

Figure 7. Proposed structure of Cu(II) binding with CSHQ. [Color figure can be viewed in the online issue, which is available at wileyonlinelibrary.com.]

Mechanism of the Cu(II) Sorption on CSHQ

It was noteworthy that when CS and their derivatives were used for adsorption purposes, the predominant mechanism involved between the adsorbent and adsorbate was chemisorption. To further understand the mechanism of Cu(II) adsorption onto CSHQ, FTIR spectroscopy and EDX analysis of the metal-loaded CSHQ were carried out. FTIR spectra of CSHQ before and after adsorption were obtained to identify the chemical functional groups that are involved in the adsorption of Cu(II) (Figure 1). In the IR spectra of Cu(II)-loaded CSHQ, the band at 3469 cm^{-1} corresponding to γ(OH) shifted to a lower wavelength; this indicated that Cu(II) was bound to hydroxyquinoline oxygen. This was further confirmed by the appearance of a band at 500–520 cm^{-1} due to γ(Cu—O).[66] The band around 1570 cm^{-1} in the IR spectra of CSHQ shifted to a lower region; this confirmed that the nitrogen atom of pyridine also participated in the binding of Cu(II) ions. From the FTIR spectral results, we assumed that ONN atoms in the CSHQ were involved the binding of the copper ions. The mechanism was further elucidated with EDX analysis, as shown in Figure 4 in the Supporting Information. The EDX pattern of CSHQ did not exhibit the characteristic signal of Cu(II), whereas Cu(II)-loaded CSHQ showed a clear signal of the presence of Cu(II).

Also, the experimental results of kinetic studies clearly show that Cu(II) removal by CSHQ followed the PSO rate model; this suggested that the overall process was controlled by chemisorption. In summary, the kinetics, isotherm FTIR spectroscopy, and EDX analysis suggested that the Cu(II) adsorption onto CSHQ involved a chemisorption mechanism. On the basis of the previous results, a possible mechanism between Cu(II) and CSHQ through ONN atoms is shown in Figure 7.

CONCLUSIONS

In summary, we successfully synthesized a novel CS derivative via a simple condensation process and applied it to the removal of Cu(II) from aqueous solution. The adsorption kinetics results agreed with the PSO model and the adsorption isotherm data fit the Langmuir isotherm model. The material exhibited good

performance in the removal of Cu(II) with an efficient adsorption capacity of 88.07 mg/g at pH 5. The plausible chelation mechanism was due to the formation of bonds between the Cu(II) and ONN atoms from CSHQ in a tridentate manner. The as-prepared CSHQ exhibited efficient adsorption for copper removal in water; this suggests its use as a promising material for water treatment. Further, the results outlined here could indicate that this ligand could be useful for various analytical and environmental applications.

ACKNOWLEDGMENTS

This work was supported by a National Research Foundation of Korea grant (contract grant number 2012R1A2A4A01001539) funded by the Korea government (Ministry of Education, Science, and Technology).

REFERENCES

1. Demirbaş, Ö.; Karadağ, A.; Alkan, M.; Doğan, M. *J. Hazard. Mater.* **2008**, *153*, 677.
2. Nuhoglu, Y.; Oguz, E. *Process. Biochem.* **2003**, *38*, 1627.
3. Rajiv Gandhi, M.; Kousalya, G. N.; Meenakshi, S. *Int. J. Biol. Macromol.* **2011**, *48*, 119.
4. Larous, S.; Meniai, A. H.; Lehocine, M. B. *Desalination* **2005**, *185*, 483.
5. Zhang, L.-J.; Cao, L.-Q.; Wang, X.-H.; Wang, J.-D. *Polym. Adv. Technol.* **2012**, *23*, 1174.
6. Yu, B.; Zhang, Y.; Shukla, A.; Shukla, S. S.; Dorris, K. L. *J. Hazard. Mater.* **2000**, *80*, 33.
7. Mohan, D.; Pittman, C. U., Jr.; Steele, P. H. *J. Colloid Interface Sci.* **2006**, *297*, 489.
8. Lee, S.-H.; Yang, J.-W. *Sep. Sci. Technol.* **1997**, *32*, 1371.
9. Ajmal, M.; Hussain Khan, A.; Ahmad, S.; Ahmad, A. *Water Res.* **1998**, *32*, 3085.
10. Bouzid, J.; Elouear, Z.; Ksibi, M.; Feki, M.; Montiel, A. *J. Hazard. Mater.* **2008**, *152*, 838.
11. Reddy, D.; Lee, S.-M.; Seshaiah, K. *Water Air Soil Pollut.* **2012**, *223*, 5967.
12. Crini, G. *Prog. Polym. Sci.* **2005**, *30*, 38.
13. Pontoni, L.; Fabbricino, M. *Carbohydr. Res.* **2012**, *356*, 86.
14. Muzzarelli, R. A. A. *Carbohydr. Polym.* **2011**, *84*, 54.
15. Bhatnagar, A.; Sillanpää, M. *Adv. Colloid Interface Sci.* **2009**, *152*, 26.
16. Wu, F.-C.; Tseng, R.-L.; Juang, R.-S. *J. Environ. Manage.* **2010**, *91*, 798.
17. Miretzky, P.; Cirelli, A. F. *J. Hazard. Mater.* **2009**, *167*, 10.
18. Gerente, C.; Lee, V. K. C.; Cloirec, P. L.; McKay, G. *Crit. Rev. Env. Sci. Technol.* **2007**, *37*, 41.
19. Crini, G.; Badot, P.-M. *Prog. Polym. Sci.* **2008**, *33*, 399.
20. Elwakeel, K. Z. *J. Dispersion Sci. Technol.* **2010**, *31*, 273.
21. Zheng, Y.; Wang, A. *J. Hazard. Mater.* **2009**, *171*, 671.
22. Ngah, W. S. W.; Musa, A. *J. Appl. Polym. Sci.* **1998**, *69*, 2305.
23. Gamage, A.; Shahidi, F. *Food Chem.* **2007**, *104*, 989.
24. Miretzky, P.; Cirelli, A. F. *J. Fluorine Chem.* **2011**, *132*, 231.
25. Kyzas, G. Z.; Lazaridis, N. K. *J. Colloid Interface Sci.* **2009**, *331*, 32.
26. Jiang, R.; Fu, Y.-Q.; Zhu, H.-Y.; Yao, J.; Xiao, L. *J. Appl. Polym. Sci.* **2012**, *125*, E540.
27. Cestari, A. R.; Vieira, E. F. S.; Pinto, A. A.; Lopes, E. C. N. *J. Colloid Interface Sci.* **2005**, *292*, 363.
28. Chiou, M.-S.; Ho, P.-Y.; Li, H.-Y. *Dyes Pigments* **2004**, *60*, 69.
29. Wan Ngah, W. S.; Teong, L. C.; Hanafiah, M. A. K. M. *Carbohydr. Polym.* **2011**, *83*, 1446.
30. Burkhardt, A.; Görls, H.; Plass, W. *Carbohydr. Res.* **2008**, *343*, 1266.
31. Wang, L.; Li, Q.; Wang, A. *Polym. Bull.* **2010**, *65*, 961.
32. Moore, G. K.; Roberts, G. A. F. *Int. J. Biol. Macromol.* **1981**, *3*, 337.
33. Muzzarelli, R.; Baldassarre, V.; Conti, F.; Ferrara, P.; Biagini, G.; Gazzanelli, G.; Vasi, V. *Biomaterials* **1988**, *9*, 247.
34. Antony, R.; Theodore David, S.; Saravanan, K.; Karuppasamy, K.; Balakumar, S. *Spectrochim. Acta Part A* **2013**, *103*, 423.
35. Rodrigues, C. A.; Laranjeira, M. C. M.; de Fávere, V. T.; Stadler, E. *Polymer* **1998**, *39*, 5121.
36. dos Santos, J. E.; Dockal, E. R.; Cavalheiro, É. T. G. *Carbohydr. Polym.* **2005**, *60*, 277.
37. Krishnapriya, K. R.; Kandaswamy, M. *Carbohydr. Res.* **2009**, *344*, 1632.
38. Krishnapriya, K. R.; Kandaswamy, M. *Carbohydr. Res.* **2010**, *345*, 2013.
39. Zalloum, H. M.; Al-Qodah, Z.; Mubarak, M. S. *J. Macromol. Sci. Pure Appl. Chem.* **2008**, *46*, 46.
40. Zhang, H.; Thomas, R.; Oupicky, D.; Peng, F. *J. Biol. Inorg. Chem.* **2008**, *13*, 47.
41. Liu, Y.-C.; Yang, Z.-Y. *J. Biochem.* **2010**, *147*, 381.
42. Liu, Y.-C.; Yang, Z.-Y. *Eur. J. Med. Chem.* **2009**, *44*, 5080.
43. Arslan, T.; Öğretir, C.; Tsiouri, M.; Plakatouras, J. C.; Hadjiliadis, N. *J. Coord. Chem.* **2007**, *60*, 699.
44. Brunel, F.; El Gueddari, N. E.; Moerschbacher, B. M. *Carbohydr. Polym.* **2013**, *92*, 1348.
45. de Britto, D.; Assis, O. B. G. *Carbohydr. Polym.* **2007**, *69*, 305.
46. Anan, N. A.; Hassan, S. M.; Saad, E. M.; Butler, I. S.; Mostafa, S. I. *Carbohydr. Res.* **2011**, *346*, 775.
47. Trimukhe, K. D.; Varma, A. *J. Carbohydr. Polym.* **2008**, *71*, 698.
48. Qin, Y.; Liu, S.; Xing, R.; Yu, H.; Li, K.; Meng, X.; Li, R.; Li, P. *Carbohydr. Polym.* **2012**, *89*, 388.
49. Ho, Y.-S. *J. Hazard. Mater.* **2006**, *136*, 681.
50. Lagergren, S. *Handlingar* **1898**, *24*, 1.
51. Ho, Y. S.; McKay, G. *Process. Biochem.* **1999**, *34*, 451.
52. Ho, Y.-S. *Water Res.* **2006**, *40*, 119.
53. Weber, W. J.; Morris, J. C. *J. Sanit. Eng. Div. Am. Soc. Civ. Eng.* **1963**, *89*, 31.

54. Poots, V. J. P.; McKay, G.; Healy, J. *J. Water Res.* **1976**, *10*, 1061.
55. Langmuir, I. *J. Am. Chem. Soc.* **1916**, *38*, 2221.
56. Hall, K. R.; Eagleton, L. C.; Acrivos, A.; Vermeulen, T. *Ind. Eng. Chem. Fundam.* **1966**, *5*, 212.
57. Freundlich, H. Z. *Phys. Chem.* **1906**, *57*, 385.
58. Adamson, A. W.; Gast, A. P. Physical Chemistry of Surfaces; Wiley: New York, **1990**.
59. Sips, R. *J. Chem. Phys.* **1948**, *16*, 490.
60. Rajiv Gandhi, M.; Kousalya, G. N.; Viswanathan, N.; Meenakshi, S. *Carbohydr. Polym.* **2011**, *83*, 1082.
61. Wan Ngah, W. S.; Endud, C. S.; Mayanar, R. *React. Funct. Polym.* **2002**, *50*, 181.
62. Vasconcelos, H. L.; Guibal, E.; Laus, R.; Vitali, L.; Fávere, V. T. *Mater. Sci. Eng. C* **2009**, *29*, 613.
63. Justi, K. C.; Fávere, V. T.; Laranjeira, M. C. M.; Neves, A.; Peralta, R. A. *J. Colloid Interface Sci.* **2005**, *291*, 369.
64. Laus, R.; de Fávere, V. T. *Bioresour. Technol.* **2011**, *102*, 8769.
65. Kannamba, B.; Reddy, K. L.; AppaRao, B. V. *J. Hazard. Mater.* **2010**, *175*, 939.
66. Chikate, R. C.; Belapure, A. R.; Padhye, S. B.; West, D. X. *Polyhedron* **2005**, *24*, 889.